Available online at www.sciencedirect.com
ScienceDirect
Trans. Nonferrous Met. Soc. China 28(2018) 642−650
Transactions of Nonferrous Metals Society of China
www.tnmsc.cn

Comparative study on corrosion behaviors of Mg−Al−Zn alloys

Sennur CANDAN, Ercan CANDAN

Department of Mechanical and Manufacturing Engineering, Bilecik Seyh Edebali University, Bilecik, Turkey

Received 17 February 2017; accepted 2 July 2017

Abstract: A comparative study on corrosion behaviors of various Mg−Al−Zn alloys (AZ21, AZ41, AZ61 and AZ91 series, cast under same cooling conditions and controlled alloying composition) was carried out. Scanning electron microscopy (SEM) and X-ray diffraction (XRD) were used for microstructural examinations. The corrosion behaviors were evaluated by immersion tests and potentiodynamic polarization measurements in 3.5% NaCl solution. The results showed that the influence of Al addition on corrosion resistance was more pronounced up to 4% (i.e. AZ41) above which its influence was at less extent. The deterioration of the corrosion resistance of the alloys, at higher Al contents, was attributed to the amount and morphology of β-$Mg_{17}Al_{12}$ intermetallics and the interruption of continuity of the oxide film on the surface of the alloys owing to coarsened β intermetallics.

Key words: Mg alloy; AZ series alloys; casting; corrosion

1 Introduction

Aluminum-containing magnesium alloys (AZ, AM, AS series) are particularly attractive for aerospace and automotive industries due to their low densities [1−4]. Among the magnesium alloys, AZ series magnesium alloys are the most successfully used commercial alloys in the manufacturing industry, which contain Al, Zn and a small quantity of Mn [4]. However, the application of the AZ series magnesium alloys is still limited owing to its limited strength and lower corrosion resistance as compared with the aluminium alloys [5].

It is well known that formation of β-intermetallic ($Mg_{17}Al_{12}$) precipitates at the grain boundaries takes place in Mg alloys above 2% Al content [3,6]. The morphology of β intermetallic is mainly depended upon the volume fraction of Al [7−9], solidification rate of the melt [10,11] and minor alloying additions [12−16].

A number of studies have been published on AZ series Mg alloys to understand their corrosion mechanisms [6−8,17−24]. However, the controversial views on the role of Al for the corrosion of AZ series magnesium alloy still exist. According to some researchers [17,18], the corrosion resistance of magnesium alloy improves in a noticeable level when aluminum content reaches 8%−9% due to protective barier effect of β-intermetallic promoted by Al content, while, some other researchers [6,7,23,24] reported that the β-intermetallics may not act as a protective barrier but may act as a micro-galvanic cells with the alloy matrix leading to an increased corrosion. In Refs [8,20,21], the corrosion resistance of AZ91 alloy, which contains 9% Al, is better than that of AZ21 or AZ31 alloys. PARDO et al [8] examined the influence of aluminium content of AZ31, AZ80 and AZ91D alloys and concluded the barier effect of β-intermetallic due to increased Al content in AZ91 alloy. WANG et al [22] reported that corrosion resistance of AZ61 alloy is better comapred with that of AZ31 alloy. Some researchers [8,20−22] observed two key factors for the lowest corrosion rates for AZ91 alloy, the aluminium enrichment on the corroded surfaces and the β-intermetallic which acted as a barrier for the corrosion progress. Unlike the studies above, some other researchers [6,7,23,24] reported that the β-intermetallic may not act as a protective barrier but may act as a micro-galvanic cells with the alloy matrix. They concluded that intensity of the galvanic corrosion appears to be quite higher for AZ91 alloy compared with that of AZ21 or AZ31 alloys owing to increased amount of the β-intermetallic in AZ91 alloy which acted as micro-galvanic cells.

Although, aforementioned studies [7,8,20−24] dealt with corrosion behaviors of AZ series Mg alloys, these studies were carried out in a non-systematic manner.

Corresponding author: Sennur CANDAN; E-mail: sennur.candan@bilecik.edu.tr
DOI: 10.1016/S1003-6326(18)64696-5

For example, AZ31 and/or AZ61 alloys were compared with AZ91 alloy [8,22] and discussed in the frame of their Al content ignoring their production method. In the studies [8,22], AZ91 alloy was obtained in the form of billet and AZ31 alloy was in the form of rolled plate. It is well known that alloying elements [12−16], cooling conditions [10,11] and production methods (i.e cast, rolled, etc.) overwhelmingly affect the microstructure and, therefore, the corrosion resistance of the alloys. The controversial views above on the role of Al on the corrosion of AZ series magnesium alloy still exist. Therefore, the purpose of the present work is to better understand the influence of Al on the corrosion behaviors of various AZ series Mg alloys (AZ21, AZ41, AZ61 and AZ91) cast under similar cooling conditions and controlled alloying compositions.

2 Experimental

Mg (99.99%), Al (99.99%) and Zn (99,98) ingots were used as starting materials. Master alloys were prepared by melting pure Mg together with pure Al in an electrical furnace under Ar gas atmosphere at 750 °C and cast as ingot form. Zn addition was carried out for 1 min before the casting to avoid loss of Zn due to vaporization. The master alloy was then remelted and cast into a preheated cast iron mold (250 °C) under protective SF_6 gas with a cooling rate of 5 °C/s. The alloy specimens were used in as-cast form. AZ01 alloy, which contained no Al, was also prepared as control sample. The chemical compositions of the alloys, determined by using Spectrolab M8 optical emission spectrometry (OES), are given in Table 1. Microstructural evaluations were carried out by scanning electron microscopy (SEM). Samples having 15 mm in diameter and 10 mm in length were machined and subsequently ground from 220 to 1200 grit emery papers followed by polishing with 1 μm diamond paste for the immersion tests and microstructural evaluations. For SEM investigations of AZ01, AZ21 and AZ41, polished samples were etched in acetic-picral for a few seconds and for AZ61 and AZ91 alloys, 2% nital was used. X-ray diffraction (XRD) analysis (Philips RV 3710 X-ray diffractometer) was carried out under Cu K_α radiation with the incidence beam angle of 2°.

Table 1 Chemical composition of AZ series magnesium alloys used (mass fraction, %)

Alloy	Al	Mn	Zn	Fe	Mg
AZ01	0.4	0.28	1.22	0.002	Bal.
AZ21	1.9	0.22	1.30	0.002	Bal.
AZ41	4.3	0.26	1.11	0.002	Bal.
AZ61	6.3	0.25	0.93	0.002	Bal.
AZ91	9.5	0.21	0.84	0.002	Bal.

Two different immersion tests were employed: one was for mass loss measurements and the other was for observation of initial stage of the oxide film on the surface of the samples. For the mass loss measurements, the polished samples were weighed and then immersed in 3.5% NaCl solution for 72 h. After the immersion tests, the samples were cleaned with a solution containing 200 g/L CrO_3 for 15 min to remove the corrosion products. Finally, they were cleaned with distilled water, dried and weighed. The mass losses of the samples were then normalized in the unit of mg/(cm^2·d) by considering the total surface area of the samples. For the observation of the initial stage of the oxide film, the polished samples were immersed in 3.5% NaCl solution for 0.25 h then ultrasonically cleaned in distilled water and left to dry at room temperature.

For the potentiodynamic polarization measurements, machined samples of 9 mm × 9 mm × 9 mm were connected to copper wire and embedded in an epoxy resin holder. The surfaces were then abraded up to 1200 mesh emery paper, mechanically polished down to 1 μm diamond paste and washed and ultrasonically rinsed in distilled water. The potentiodynamic curves were performed by means of a Gamry model PC4/300mA potentiostat/galvanostat controlled by a computer with DC105 mass analysis software. The embedded specimens in epoxy resin were utilized as working electrodes. A carbon rod (6 mm in diameter) and a saturated calomel electrode (SCE) were used as a counter electrode and reference electrode, respectively. Experiments were performed at room temperature in a glass cell containing 3.5% NaCl solution. Each polarization experiment was carried out holding the electrode for 45 min at open circuit potential (φ_o) to allow steady-state is to be achieved. Potentiodynamic polarization curves were generated by sweeping the potential from cathodic to anodic direction at a scan rate of 1 mV/s, starting from −2.00 up to 0.20 V. Each data point for both immersion and potentiodynamic polarization tests represents at least average of three different measurements.

3 Results and discussion

3.1 Microstructure

The microstructures of the examined AZ series Mg alloys are shown in Fig. 1. The microstructure consisted of primarily Mg-rich solid solution and secondary intermetallics both at the grain boundaries and occasionally within the α-Mg grains. The XRD analysis indicated that AZ21, AZ41, AZ61 and AZ91 alloys mainly consisted of α-Mg solid solution and the

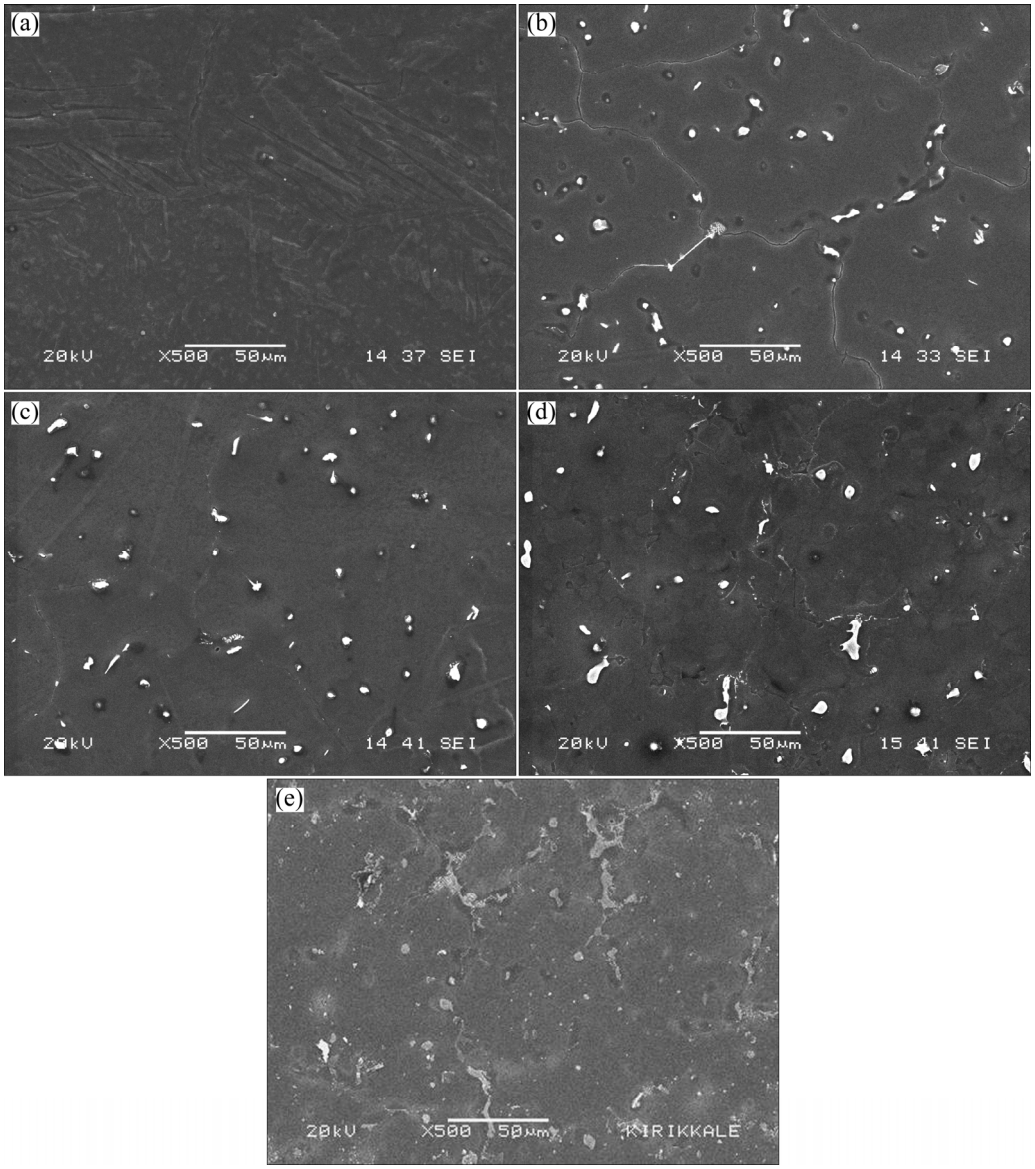

Fig. 1 SEM micrographs of AZ01 (a), AZ21 (b), AZ41 (c), AZ61 (d) and AZ91 (e) series Mg alloys

compound of intermetallic β-$Mg_{17}Al_{12}$ phases (Fig. 2). Patterns for AZ41 and AZ61 alloys were not included in Fig. 2 for clarity but their patterns sit between AZ21 and AZ91 alloys. High magnification SEM micrograph and EDS analysis of AZ21 are shown in Fig. 3 and Table 2, respectively. The EDS micro analyses in Fig. 3 and Table 2, confirm that the bright second phase particle (marked as 1) contains mainly Mg−Al−Mn−Zn elements and continuous phase alongside the grain boundaries contains Mg−Al elements (marked as 2). The bright phase was believed to be Al−Mn phases [25−27]. PAN et al [25] reported that there were two types of compounds in the AZ61 alloy, i.e., Al_8Mn_5 and $Al_{11}Mn_4$. The former existed as particles, and the latter was formed as needle, angular particle and flower shape distributing mainly at the interdendritic boundaries and few in the α-Mg matrix. The intermetallic phases had been progressively inreased with the increasing Al content (i.e AZ61 and

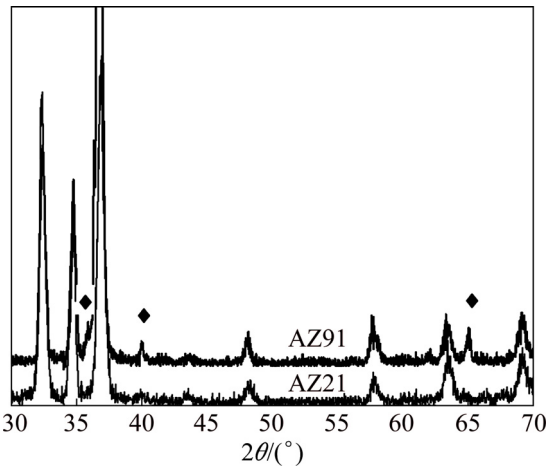

Fig. 2 XRD patterns of AZ21 and AZ91 alloys (The peaks marked with a diamond are from β-$Mg_{17}Al_{12}$ and all other peaks are from α-Mg)

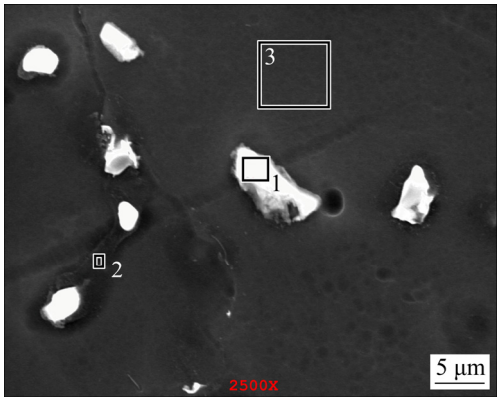

Fig. 3 SEM micrograph of AZ21 alloy (The numbers indicated on the micrograph represent the places where EDS measurement was carried out)

Table 2 EDS results of studied alloys in Fig. 3 (mass fraction, %)

Location	Al	Mn	Zn	Mg
1	21.03	12.29	7.09	59.58
2	9.33			90.67
3	1.50			98.50

AZ91) and transformed to a coarsened net-like structure (Figs. 1(d) –(e)). According to the Mg−Al equilibrium phase diagram, the eutectic β is expected to appear when the Al content reaches ~13%. However, the eutectic β intermetallic appears in alloys containing above 2% Al in nonequilibrium cooling conditions normally encountered in Mg alloy castings [3,6,28]. In higher Al-containing alloys (i.e AZ61 and 91), lamellar and partially divorced β eutectics appear (Fig. 4). As reported previously [12,14,29], the eutectic with the lamellar structure in AZ91 Mg alloy is formed adjacent to the partially divorced eutectics in accord with the present work. It should mentioned that some of the Al−Mn phases were believed to be embedded in the clustered β intermetallics. PAN et al [25] reported that a number of Al−Mn particles were present in the β phases, which had been proved as Al_8Mn_5.

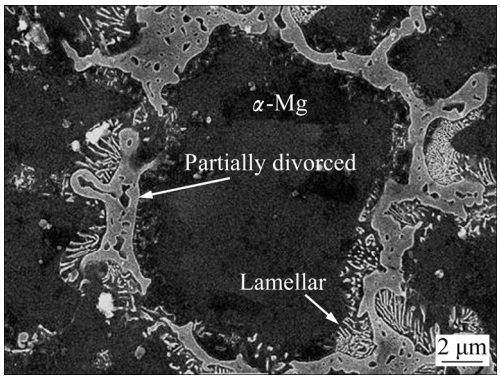

Fig. 4 High magnification SEM morphology of secondary intermetallics in AZ91 alloy

3.2 Corrosion

Figure 5 illustrates the results of mass loss from the immersion tests. The mass loss was calculated by proportioning the mass change before and after corrosion to the sample surface area. Evidently, mass loss of the samples decreased immediately after addition of Al compared with non-Al-containing alloy (i.e AZ01). However, the influence of Al addition was more pronounced up to 4% (i.e AZ41) above which its influence was at less extent. Compared with AZ01 control alloy, the mass loss decreased nearly four fold in AZ41 alloy.

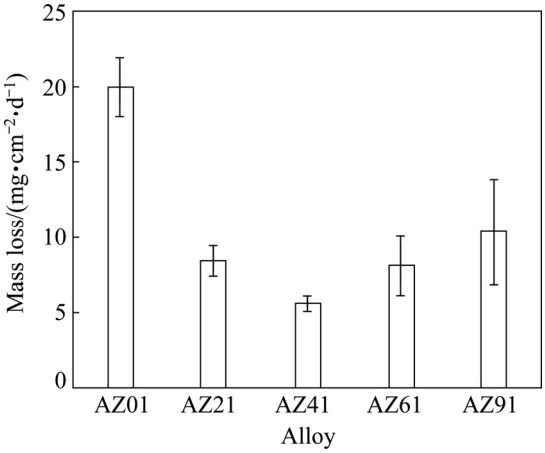

Fig. 5 Mass loss of AZ series Mg alloys obtained from 72 h immersion test in 3.5% NaCl solution

Cross section SEM images of the samples, immersed in 3.5% NaCl for 72 h, are shown in Fig. 6. Representative areas of the cross-sections immediately starting from the corroded surface to the inner part of the sample are illustrated in Fig. 6. The corrosion had propagated from the surface through inner part of the alloy, and many deep corrosion pits on the surface of the alloys took place. Evidently, AZ41 alloys exhibited much better corrosion resistance compared with those of the AZ61 and AZ91 alloys, indicating that the alloys containing higher Al contents (>4.0%) are subjected to a higher localized breakdown. The corrosion attack at the samples made of AZ91 alloy was tremendous that the corrosion, in some part of the samples, had been propagated through inner part of the AZ91 alloy by following the β intermetallic network as shown in Fig. 6(e).

Figure 7 shows potentiodynamic polarization curves of five AZ series magnesium alloys studied. Their φ_{corr}, J_{corr} values (obtained from Tafel-type fit technique) and calculated corrosion rates (CR) are summarised in Table 3. The corrosion rate (CR) conversions were carried out as suggested in Ref. [30]. Compared with AZ01 control alloy, J_{corr} value of the AZ41 alloy decreased from 65.86 to 3.16 μA/cm^2 respectively. The

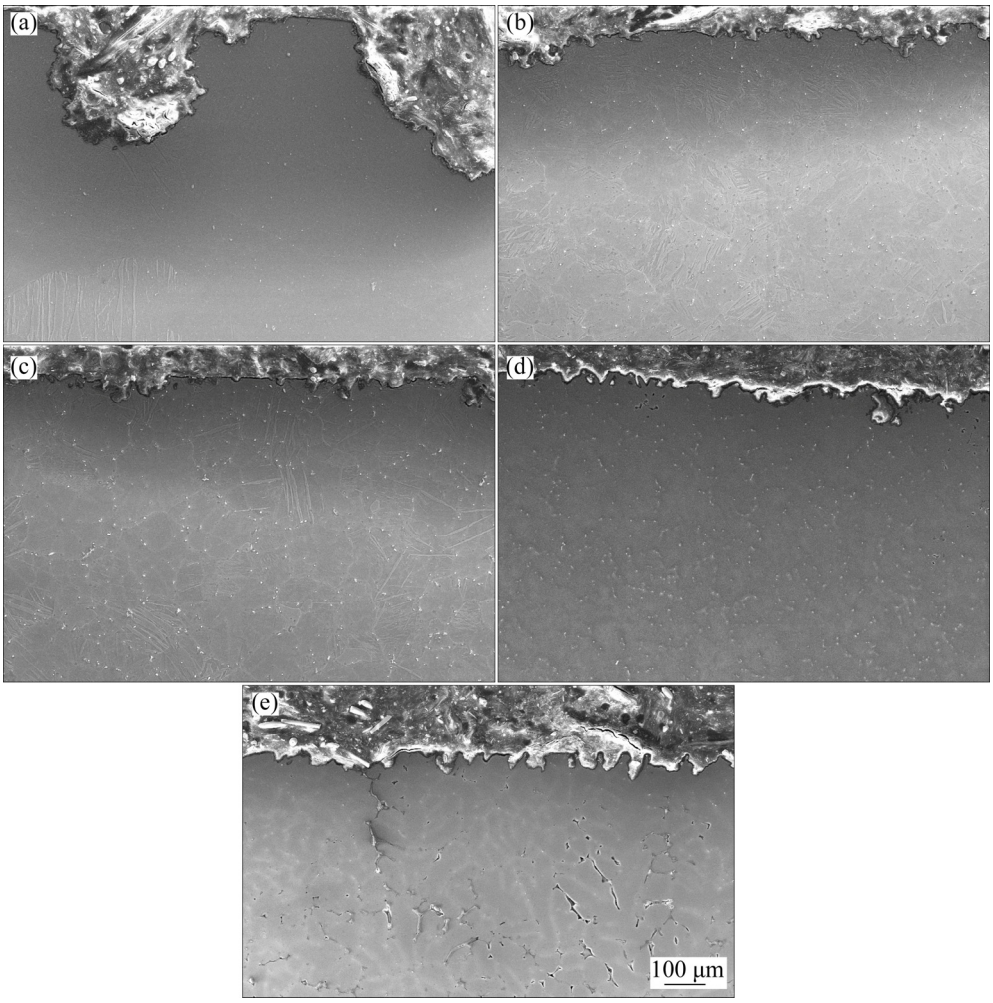

Fig. 6 SEM micrographs showing cross section of AZ01 (a), AZ21 (b), AZ41 (c), AZ61 (d) and AZ91 (e) Mg alloys immersed in 3.5% NaCl solution for 72 h

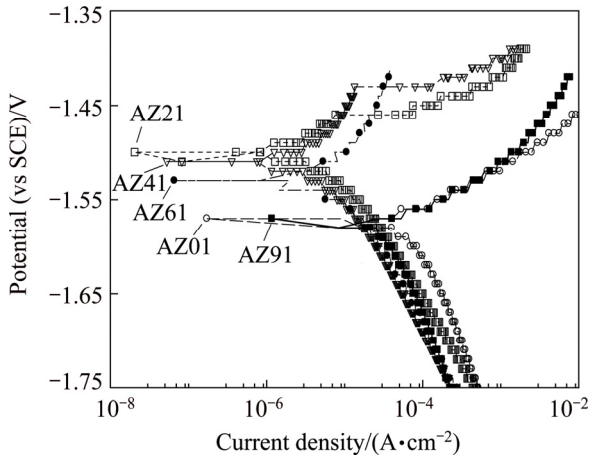

Fig. 7 Potentiodynamic polarization curves for AZ series Mg alloys in 3.5% NaCl environment

J_{corr} difference between AZ21 and AZ41 is relatively small (i.e 5.74 and 3.16 μA/cm^2 respectively) while it increases from 3.16 to 36 μA/cm^2 for AZ41 and AZ91 alloys respectively. The results in Table 3 are very much in line with the mass loss results in Fig. 5.

Table 3 φ_{corr}, J_{corr} and CR values of AZ series Mg alloys derived from polarization curves

Alloy	φ_{corr} (vs SCE)/ mV	J_{corr}/ (μA·cm^{-2})	CR/ (mm·a^{-1})
AZ01	−1571	65.86	1.51
AZ21	−1501	5.74	0.13
AZ41	−1511	3.16	0.07
AZ61	−1531	9.8	0.22
AZ91	−1573	36.0	0.82

It is well known that the corrosion is strongly dependent on the aluminium content and microstructure of Mg alloys [7−11]. The influences affecting the corrosion of AZ series alloys are; Al content, the grain size of the α-matrice, extend and the morphology of intermetallics, soldification rate of the melt and/or minor alloying additions, the oxide film on the surface of Mg alloys [7−21,31,32]. Compared with AZ01 control alloy, better corrosion resistances of AZ21, AZ41, AZ61 and AZ91 alloys are attributed to Al content of Mg alloy.

However, the influence of Al addition was more pronounced up to 4% (i.e AZ41) above which its influence was at less extent. As discussed earlier in the microstructure section, as Al content of the alloy increases, the presence of β intermetallic increases and its morphology coarsens. The present study indicated that Al content of gravity cast AZ series Mg alloys should be around 4% in order to avoid coarsening of β intermetallics in agreement with the work of WARNER et al [19] who reported that even 5% addition of Al in magnesium alloy is beneficial for improving their corrosion resistance. However, some other researchers [17,19] reported that the corrosion resistance of magnesium alloy improves in a noticeable level when aluminum content reaches 8%−9%. These discrepancies may arise from the composition of the alloys and/or casting conditions (casting temperature, solidification rate, etc.). Our previous studies [11,12,14] as well as other studies [16] showed that solidification rate of the melt and minor alloying additions considerably alter the grain size of the alloy, morphology and distribution of the β intermetallics, therefore, the corrosion resistance of the AZ91 alloys. Based on the galvanic corrosion principles, a higher amount of cathode (intermetallics) in relation to the size of the anode (α-Mg) results in an increased galvanic corrosion. Indeed, the highest mass loss is observed in AZ91 alloy since the ratio of the β intermetallics in AZ91 is higher than that of AZ21, AZ41 and AZ61 alloys. Similar results have also been reported by Refs. [23,24] for AZ31 and AZ91 alloys. Contrarily, Refs. [8,21] reported that corrosion resistance of AZ91 alloy was better than AZ31 alloy. These improvements are attributed to the barrier effect of β intermetallics [8,21]. However, all of these works [8,21] have been carried out by using electrochemical tests and not supported by long term immersion tetst (i.e >24 h). It has been stated [33] that short-term corrosion tests to provide corrosion rates for Mg alloys do not agree with long-term tests. Often, the corrosion rate of Mg evaluated from Tafel extrapolation has pertained to conditions soon after specimen immersion and these corrosion rates have not related to steady state corrosion.

The influence of Al in Mg alloys on the oxidation behaviour in various media has been studied extensively [7,31]. In aqueous media, the oxide film on the surface of Mg and its alloys is formed as quasi-passive form of $Mg(OH)_2$. This $Mg(OH)_2$ film is porous [5] and not fully protective, therefore, it is destroyed because of existence of Cl^- at prolonged exposure time [34]. The addition of Al to Mg modifies the oxide film on the surface and the microstructure improving its resistance to the aggressive attack of Cl^- ions. SONG et al [32] proposed formation of oxide film on AZ91 alloys. The film consisted of three layers: an inner layer (rich in Al_2O_3), a middle layer (mainly MgO) and an outer layer ($Mg(OH)_2$). More recently, ESMAILY et al [35] reported that Al enrichment in the inner part of the film on AZ91 alloy was evident and Al was in the oxidized state. SONG et al [32] and ESMAILY et al [35] suggested that the positive effect of Al in Mg alloy on corrosion properties was due to the protective properties of the Al-enriched layer at the inner part of the film (i.e. formation of Al_2O_3 layer at the inner part may act as a passive film between the quasi-passive film and the surface of the alloy). Although, Al contents of AZ61 and AZ91 alloys are higher than that of AZ41 alloy, their higher mass loss may be due to discontinuity of the oxide film in the regions where relatively coarsened β intermetallics are present. The interruption of the continuity of the oxide film on the surface of the alloy, owing to formation of the coarsened intermetallics, is evident as shown in Figs. 8(d,e). The hydration of the MgO occurs as exposed to water. The hydration of the MgO converts the cubic MgO to hexagonal $Mg(OH)_2$ having a volume twice that of the oxide leading to a considerable disruption of the film and the formation of regions of charge instability [31]. On the other hand, oxide film on β intermetallics form as $AlMg_x(OH)_y$ and the film growth rates on the β intermetallics are much faster than those on α-Mg [31]. Differencies in volume changes between the two different oxides (i.e $Mg(OH)_2$ and $AlMg_x(OH)_y$) may distrupt the interface between α-Mg and the β intermetallics. This is schematically illustrated in Fig. 9. Compressive ruptures of the film may take place resulting in continual exposure of fresh metal surface leading to a prolonged corrosion [31]. SAMANIEGO et al [23] stated that in contrast with the beneficial effect of Al, higher Al-containing Mg alloys, with appreciable amounts of β intermetallic, may corrode faster than alloys of lower Al content if the protective effect of the preexisting surface oxide film is lost. In the present work, propagation of the corrosion by following the intermetallic network in the microstructure is evident (Fig. 6(e)), which is attributed to disruption of the oxide film supporting the argument above.

4 Conclusions

1) Microstructure of the AZ series Mg alloys is composed of α-Mg matrix, Al−Mn and β-$Mg_{17}Al_{12}$ intermetallics. As Al content of the alloys increases (>4%), the globular shaped β intermetallic is transformed into a more coarsened lamellar or partially divorced β eutectics.

2) The results, from both the immersion tests and the potentiodynamic polarization measurements, show that AZ41 alloy exhibits better corrosion resistance

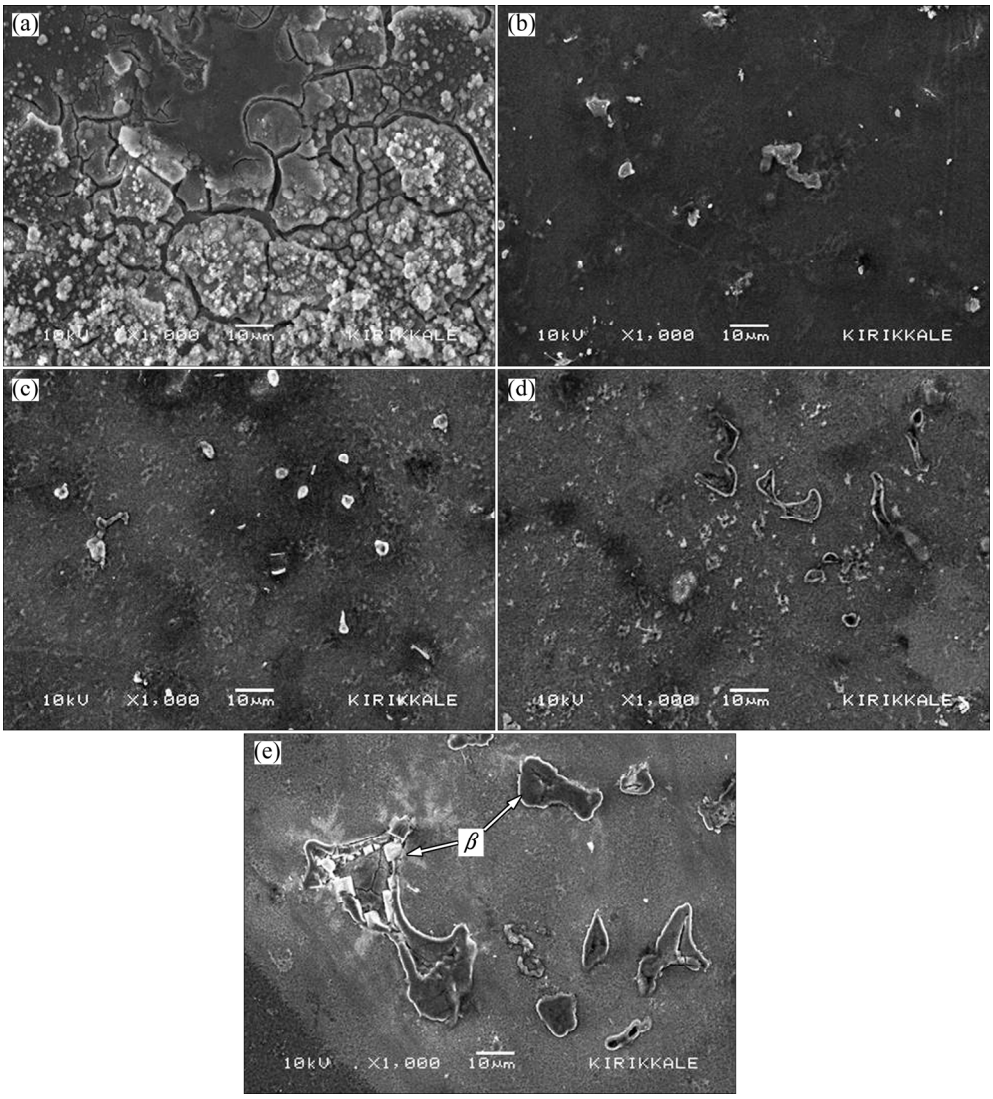

Fig. 8 Surface morphologies showing oxide film on AZ01 (a), AZ21 (b), AZ41 (c), AZ61 (d) and AZ91 (e) alloys, immersed in 3.5% NaCl for 0.25 h

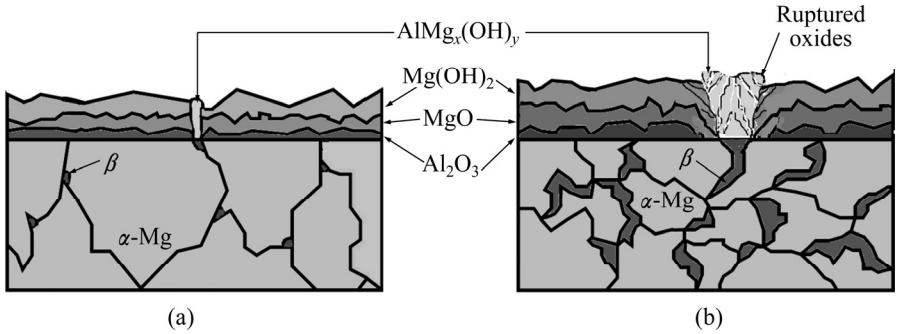

Fig. 9 Schematic illustration of oxide films on AZ21 and AZ41 (a) and AZ61 and AZ91 (b)

compared with those of the AZ21, AZ61 and AZ91 alloys.

3) The corrosion attack at the samples made of AZ91 alloy is intense, which is attributed to the influence of the morphology of β intermetallic and the interruption of the continuity of oxide film on the surface of the alloys owing to coarsened β intermetallics.

Acknowledgments

The authors are grateful for the help of Professor Harun Mindivan and Associate Professor Birol Akyuz for their laboratory facilities.

References

[1] FRIEDRICH H E, MORDIKE B L. Magnesium technology metallurgy, design data, applications [M]. 1st ed. Berlin: Springer-Verlag, 2006.

[2] LUO A A, SACHDEV A K. Applications of magnesium alloys in automotive engineering [M]//BETTLES C, BARNETT M. Advances in Wrought Magnesium Alloys. Cambridge, UK: Woodhead Publishing Limited, 2012: 393−426.

[3] PEKGULERYUZ M. Alloying behavior of magnesium and alloy design [M]//PEKGULERYUZ M O, KAİNER K U, KAYA A A. Fundamentals of Magnesium Alloy Metallurgy. Cambridge, UK: Woodhead Publishing Limited, 2013: 152−196.

[4] MANUEL M V, SINGH A, ALDERMAN M, NEELAMEGGHAM NR. Magnesium technology 2015 [C]//MANUEL M V, SINGH A, ALDERMAN M, NEELAMEGGHAM N R. Orlando, Florida, USA: Wiley-TMS Publishing, 2015.

[5] GHALI E. Corrosion resistance of aluminum and magnesium alloys, understanding, performance and testing [M]. 1st ed. New Jersey: Wiley Publishing, 2010.

[6] CHENG Ying-liang, QIN Ting-wei, WANG Hui-min, ZHANG Zhao. Comparison of corrosion behaviors of AZ31, AZ91, AM60 and ZK60 magnesium [J]. Transactions of Nonferrous Metals Society of China, 2009, 19: 517−524.

[7] SONG Guang-ling, ATRENS A, WU Xian-liang, ZHANG Bo. Corrosion behaviour of AZ21, AZ501 and AZ91 in sodium chloride [J]. Corrosion Science, 1998, 40: 1769−1791.

[8] PARDO A, MERINO M C, COY A E, VIEJO F, ARRABAL R, FELIÚ S Jr. Influence of microstructure and composition on the corrosion behaviour of Mg/Al alloys in chloride media [J]. Electrochimica Acta, 2008, 53: 7890−7902.

[9] CANDAN S, CANDAN E. A Comparative study on corrosion of Mg−Al−Si alloys [J]. Transactions of Nonferrous Metals Society of China, 2017, 27: 1725−1734.

[10] TANVERDI A. Effect of solidification rate and Si and Y additions on corrosion behavior of AZ91 Mg alloy [D]. Eskisehir: Institute of Science and Technology, Osmangazi University, 2005.

[11] CANDAN S, CELIK M, CANDAN E. Effectiveness of Ti-micro alloying in relation to cooling rate on corrosion of AZ91 Mg Alloy [J]. Journal of Alloys and Compounds, 2016, 672: 197−203.

[12] CANDAN S, UNAL M, TURKMEN M, KOC E, TUREN Y, CANDAN E. Improvement of mechanical and corrosion properties of magnesium alloy by lead addition [J]. Materials Science and Engineering A, 2009, 501: 115−118.

[13] ZENG Rong-chang, ZHANG Jin, HUANG Wei-jiu, DIETZEL W, KAINER K U, BLAWERT C, KE Wei. Review of studies on corrosion of magnesium alloys [J]. Transactions of Nonferrous Metals Society of China, 2006, 16: 763−771.

[14] CANDAN S, UNAL M, KOC E, TUREN Y, CANDAN E. Effects of titanium addition on mechanical and corrosion behaviours of AZ91 magnesium alloy [J]. Journal of Alloys and Compounds, 2011, 509: 1958−1963.

[15] GUSIEVA K, DAVIES C H J, SCULLY J R, BIRBILIS N. Corrosion of magnesium alloys: The role of alloying [J]. International Materials Reviews. 2015, 60: 169−194.

[16] CHOI H Y, KIM W J. The improvement of corrosion resistance of AZ91 magnesium alloy through development of dense and tight network structure of Al-rich α phase by addition of a trace amount of Ti [J]. Journal of Alloys and Compounds, 2017, 696: 736−745.

[17] LUNDER O, LEIN J E, AUNE T K, NISANCIOGLU K. The role of magnesium aluminuim ($Mg_{17}Al_{12}$) phase in the corrosion of magnesium alloy AZ91 [J]. Corrosion, 1989, 45: 741−748.

[18] HEHMANN F, FROES F H, YOUNG W. Rapid solidification of alumium, magnesium, and titanium [J]. Journal of Metals, 1987, 39(8): 14−21.

[19] WARNER T J, THORNE N A, NUSSBAUM G, STOBBS W M. A cross-sectional TEM study of corrosion initiation in rapidly solidified magnesium-based ribbon [J]. Surface and Interface Analysis, 1992, 19: 386−392.

[20] ANIK M, AVCI P, TANVERDI A, CELIKYUREK I, BAKSAN B, GURLER R. Effect of the eutectic phase mixture on the anodic behavior of alloy AZ9 [J]. Materials and Design, 2006, 27: 347−355.

[21] SALMAN S A, ICHINO R, OKIDO M. A Comparative electrochemical study of AZ31 and AZ91magnesium alloy [J]. International Journal of Corrosion, doi: 10.1155/2010/412129.

[22] WANG Lei, SHINOHARA T, ZHANG Bo-Ping. Electrochemical behaviour of AZ61 magnesium alloy in dilute NaCl solutions [J]. Materials and Design, 2012, 33: 345−349.

[23] SAMANIEGO A, LLORENTE I, FELIU S Jr. Combined effect of composition and surface condition on corrosion behaviour of magnesium alloys AZ31 and AZ61 [J]. Corrosion Science, 2013, 68: 66−71.

[24] SINGH I B, SINGH M, DAS S. A comparative corrosion behavior of Mg, AZ31 and AZ91 alloys in 3.5% NaCl solution [J]. Journal of Magnesium and Alloys, 2015, 3: 142−148.

[25] PAN Fu-sheng, FENG Zhong-xue, ZHANG Xi-yan, TANG Ai-tao. The types and distribution characterization of Al-Mn phases in the AZ61 magnesium alloy [J]. Procedia Engineering, 2012, 27: 833−839.

[26] GUSIEVA K, BIRBILIS N, HAMMOND V H, LABUKAS J P, PLACZANKIS B E. The influence of novel alloying additions on the performance of magnesium alloy AZ31B [R]. U.S. Army Research Laboratory, 2013.

[27] WANG Tian, KEVORKOV D, MOSTAFA A, MEDRAJ M. Experimental investigation of the phase equilibria in the Al−Mn−Zn system at 400 °C [J]. Journal of Materials, 2014, 2014: 1−13.

[28] KOC E. An investigation on corrosion dependent mechanical behaviours of biodegradable magnesium alloys [D]. Karabuk: Institute of Science and Technology, Karabuk University, 2013.

[29] BOBY A, SRINIVASAN A, PILLAI U T S, PAI B C. Mechanical characterization and corrosion behavior of newly designed Sn and Y added AZ91 alloy [J]. Materials and Design, 2015, 88: 871−879.

[30] ASM International. Corrosion, Metals Handbook [M]. 9th ed, vol. 13. Materials Park, OH: ASM International, 1987.

[31] LIU Ming, ZANNA S, ARDELEAN H, FRATEUR I, SCHMUTZ P, SONG Guang-ling, ATRENS A, MARCUS P. A first quantitative XPS study of the surface films formed, by exposure to water, on Mg and on the Mg−Al intermetallics: Al_3Mg_2 and $Mg_{17}Al_{12}$ [J]. Corrosion Science, 2009, 51: 1115−1127.

[32] SONG Guang-ling, ATRENS A, DARGUSCH M. Influence of microstructure on the corrosion of die cast AZ91D [J]. Corrosion Science, 1999, 41: 249−273.

[33] SHI Zhi-ming, LIU Ming, ATRENS A. Measurement of the corrosion rate of magnesium alloys using tafel extrapolation [J]. Corrosion Science, 2010, 52: 579−588.

[34] LIN Cui, LI Xiao-gang. Role of CO_2 in the initial stage of atmospheric corrosion of AZ91 magnesium alloy in the presence of NaCl [J]. Rare Metals, 2006, 25: 190−196.

[35] ESMAILY M, BLUCHER D B, SVENSSON J E, HALVARSSON M, JOHANSSON L G. New insights into the corrosion of magnesium alloys—The role of aluminum [J]. Scripta Materialia, 2016, 115: 91−95.

Mg−Al−Zn 合金腐蚀性能的对比研究

Sennur CANDAN, Ercan CANDAN

Department of Mechanical and Manufacturing Engineering, Bilecik Seyh Edebali University, Bilecik, Turkey

摘　要：对比研究各种 Mg−Al−Zn 合金(AZ21、AZ41、AZ61 和 AZ91 系列，相同冷却条件并控制合金成分)的腐蚀性能。用扫描电镜(SEM)和 X 射线衍射(XRD)分析合金的显微结构。通过浸泡实验评估其腐蚀行为，将样品浸泡入 3.5% NaCl 溶液中，测量其动电位极化曲线。结果表明，当铝含量小于或等于 4%时 (如 AZ41)，对耐腐蚀性的影响更显著，而当铝含量更高时，影响程度较低。当铝含量高于 4%时，合金的耐腐蚀性能下降，这与生成的 β-$Mg_{17}Al_{12}$ 金属间化合物的含量和形貌有关，粗大的 β 金属间化合物会破坏合金表面氧化膜的连续性。

关键词：镁合金；AZ 系列合金；铸造；腐蚀

(Edited by Xiang-qun LI)